IMAV2017-14
http://www.imavs.org/pdf/imav.2017.14

Technical paper

Landing and Take-off on/from Sloped and Non-planar Surfaces with more than 50 Degrees of Inclination

M. Tognon* and A. Franchi
LAAS-CNRS, Université de Toulouse, CNRS, Toulouse, France

ABSTRACT

This technical paper summarizes the recent experimental results concerning the challenging problem of landing and take-off on/from a sloped surface with an aerial vehicle exploiting the force provided by an anchored taut tether. A special regard is given to the practical aspects concerning the experimental part. In this manuscript we show extreme landing and take-off maneuvers on slopes with at least 50° inclination and non flat surfaces, such as, e.g., on industrial pipes.

1 INTRODUCTION

The popularity of aerial vehicles is growing day by day thanks to their versatility. Indeed they are currently used for several applications ranging from civil inspection to search and rescue. Those kinds of applications often require to land the vehicles on a sloped surface. For example, in the context of the European project *Aeroarms*[1], the aerial robot has to deploy a magnetic crawler or a sensor on industrial pipes that are often non-horizontal. Figure 1 shows an example of a tethered landing on a pipe tilted by an angle of $60°$.

Take-off and landing from/on a sloped surface requires to control both position and orientation (pitch) independently, since the last has match the inclination of the surface. This makes the task very challenging for a standard Vertical Take-off and Landing vehicle (VTOL) in a free-flight configuration. Indeed due to underactuation, VTOLs can control only the position and the yaw angle, while roll and pitch are a byproduct of the vehicle acceleration and the gravity force. The method normally used exploits the flatness of the system to plan a desired trajectory that ends in the landing spot and with the proper orientation [1]. However, the landing can not be done in a stable and safe configuration, i.e., with zero velocities and accelerations. Instead it requires an agile maneuver that has to be executed with very high precision. Indeed small tracking errors can easily lead to misses of the landing surface or to crashes. Furthermore, adhesive membranes are used to enforce the cohesion between the vehicle and the surface to reduce the chances to fly away after the contact. Those facts makes the task very complex and prone to errors and failures.

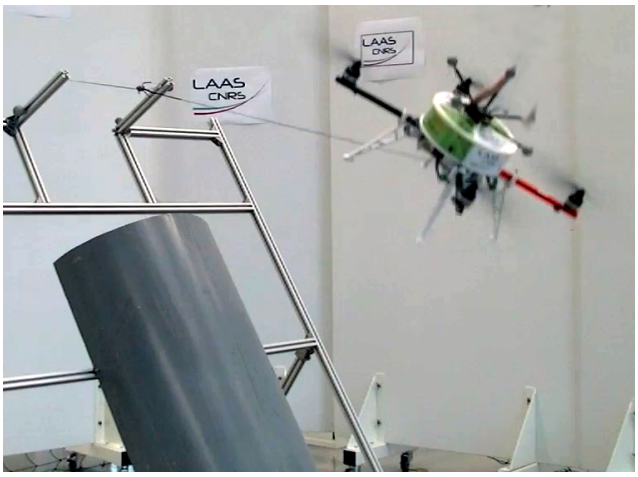

Figure 1: Tethered landing on a sloped pipe tilted by $60°$.

On the other hand, a much more reliable method gaining interest, consists on the use of a tether that connects the vehicle to a fixed point on the surface (see Fig. 1). Recent works have already studied this system, analyzing its principal properties as differential flatness, controllability and observability in the 2D case [2, 3, 4] and also in the 3D cases [5, 6, 7]. The tether, with the help of an actuated winch, has been also used in [5, 8] to land an underactuated aerial vehicle on a moving platform. Instead, in [6] we have shown that a passive tether (with no extra actuation) is enough to accomplish landing and take-off on/from sloped surfaces in a robust and reliable way.

In this paper we shall thoroughly discuss all the technical and practical aspects concerning the real execution of the landing and take-off maneuvers exploiting a tether. Here we consider a quadrotor-like vehicle and sloped surfaces tilted by at least $50°$.

2 TETHERED LANDING

In [6] we proved that the tether configuration and the inclination of the robot w.r.t. the cable are flat outputs of the system. This means that the two quantities can be precisely

*Email address(es): marco.tognon@laas.fr
[1] http://www.aeroarms-project.eu/

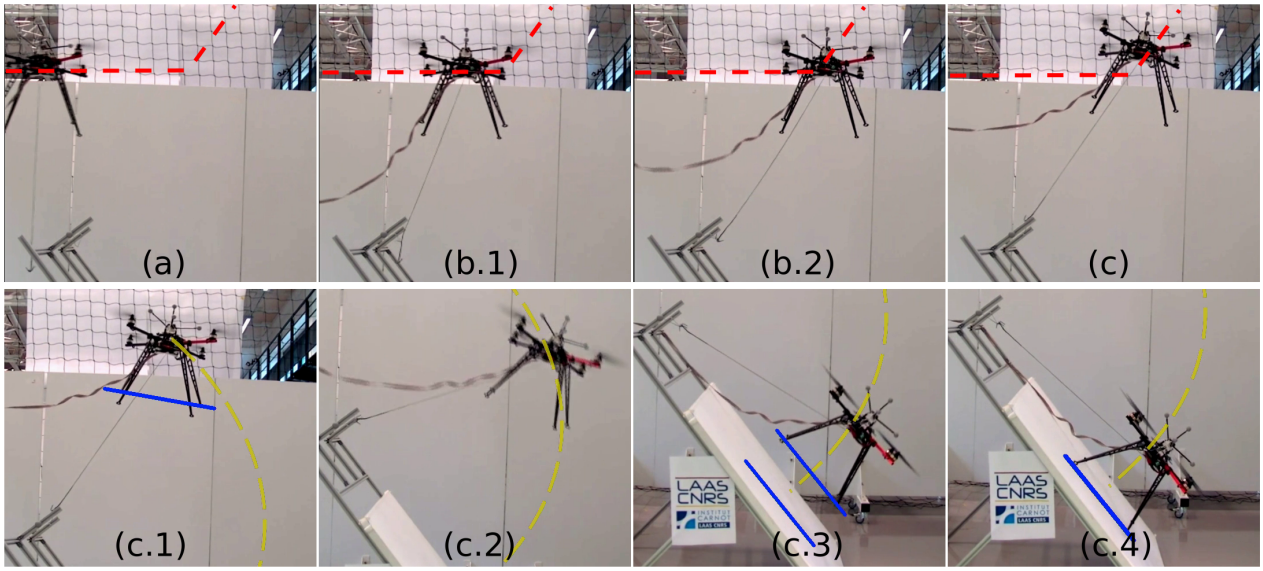

Figure 3: Sequence of images of a real experiment with a sloped surface tilted by 50°. The first row of images represents the experimental part in which the quadrotor is in a free-flight condition. In this case a standard position controller is used to track the desired position trajectory marked with a dashed red line. The second row of images represents the experimental part in which the quadrotor is tethered to the surface. In this case the controller proposed in [6] is used to track the desired position and attitude trajectories marked with a dashed yellow line and a solid blue line, respectively.

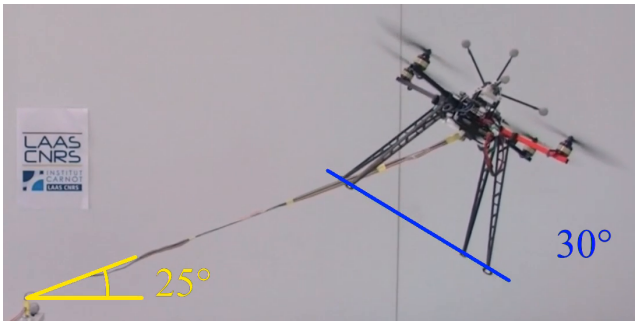

Figure 2: Inclined hovering with the robot tilted by 30° and with the cable elevation (represented in yellow) equal to 25°.

controlled in an decoupled way. In particular, thanks to the tether, the robot can hover in any point of the sphere defined by the cable constraint, with almost any orientations (not only horizontally as for the free-flight case). In particular the sphere is centered on the anchoring point and has the radius equal to the cable length. In Fig. 2 we show the robot hovering at a constant position and with an inclination of 30° with respect to the horizon.

In [6] we have shown that this property can be exploited to land the aerial robot in *inclined hovering* on any sloped surfaces. The capacity of performing the maneuver with practically zero velocity, angular velocity, acceleration, and angular acceleration makes the tethered method very robust, reliable, and safe. Thus much preferable over the free-flight method.

To control the system in [6] we designed a hierarchical controller based on the differential flatness. The controller can steer the tether configuration and the inclination of the robot along any desired trajectories. It is then used to track a spline-defined trajectory from the initial configuration to the desired landing configuration, performing the task (see Fig. 3). The take-off is done analogously.

3 Landing and Take-off on/from a Sloped Surface Tilted by 50 degrees

In this experiment we consider the plausible scenario where a quadrotor-like vehicle has to deploy a smaller robot or a sensor on a sloped surface tilted by 50°, shown in Fig. 3. The robot, equipped with a cable ending with a hook, starts from a non-tethered configuration on the ground. Therefore it has to anchor the other end of the cable to the surface to then perform the landing in a tethered configuration. Once the robot has landed on the desired spot and deployed the robot/sensor, it can take-off from the surface again exploiting the tether. Finally it can go back to the initial position after having detached the cable from the surface.

3.1 Anchoring Tools and Mechanisms

In order to pass from a free-flight configuration to a tethered one, a method to fix the end of the cable to the surface has to be found. The mechanism to do so strongly depends on the application scenario and in particular on the material of the slope. For example, in the previously mentioned scenario

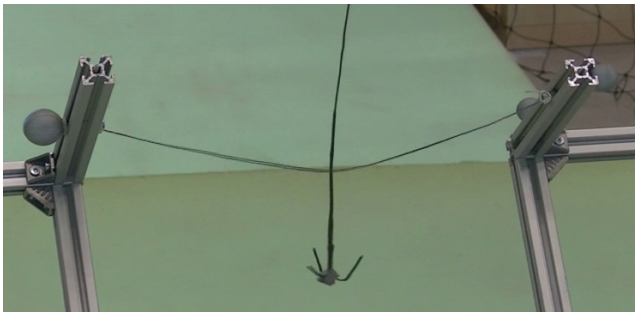

Figure 4: Zoom of the hook and the anchoring mechanism.

considered in the European project *Aeroarms*, the landing surface is mainly a pipe made of iron/steel. Thus in this case, and whenever the surface is made of proper metal, a magnetic anchor can be used to enhance the physical connection between surface and cable. In the case of a ground, snowed, or iced surface an harpoon-like mechanism might be envisaged.

In our experimental testbed we instead used a simpler solution based on a commercial fishing hook made of three tips, and an anchoring mechanism fixed to the surface made by an horizontal cable. In this way the robot can be tethered to the surface by sliding the vertical cable on the anchoring mechanism until the hook is anchored to the horizontal cable, as shown in Fig. 4. The hook can be detached from the anchoring mechanism doing the opposite operation. To facilitate this last action we increased the force pulling down the hook by slightly increasing its mass with an extra weight.

3.2 Experimental phases

Considering the previous experimental scenario and the goal, we divided the overall maneuver into several phases:

(a) approach to the anchor point with the hook,

(b) hooking of the anchoring system,

(c) stretching of the cable,

(d) tracking of the desired trajectory for tethered landing.

The phases from (a) to (c), described by the first row of images in Fig. 3, serve to pass from the initial free-flight configuration to the tethered one. Using a standard free-flight position controller and following a straight-line trajectory, the robot is able to anchor the anchoring system attached to the surface with the hook (see Fig. 3.b.2). The trajectory is planned such that the cable attached to the robot slides on the anchoring cable until the hook results attached to the last one.

Afterworld, during phase (c), the cable is stretched following a simple radial trajectory whose ending point is slightly outside the reachable region limited by the cable length. The robot, trying to reach this ending position, as explained in [9], will apply an extra force to the cable that will make it taut. In particular, the farther the desired ending position, the larger the internal force on the link. Using the dynamics of the system, the estimated state, and the control inputs, the robot can estimate the tension on the link. This estimation is then used to understand when the cable results sufficiently taut. Once the tension exceeds a certain security threshold a supervisor switches from the free-flight controller to the tethered one. Finally the planned landing trajectory is tracked. In order to compute the desired trajectories the parameters of the landing surface, such as slope angle and anchoring point, must be known. To acquire those numbers we applied some markers on the surface to measure its pose with a motion capture system. However, thanks to the robustness of the method, those parameters does not have to be very precise.

Once the robot ends the landing maneuver the take-off can start. The take-off is practically the play-back of the previous phases. Indeed, following the previous trajectory in the opposite sense lets the hook be de-attached from the anchoring mechanism to then go back to the starting point in a free-flight configuration.

3.3 Controller Switch

During the switching between the controllers, the continuity of the control input has to be guaranteed in order to preserve the stability of the system and to avoid undesired vibrations and jerks on the cable. This is obtained by setting as desired output of the next controller, the value of the system output at the switching instant. This is possible because for a specific output, there exist a unique input and state to obtain it. Therefore, asking to the next controller to remain in current state, it will requires the same input, thus preserving its continuity and the continuity of the full state.

3.4 Software Architecture

A schematic representation of the software architecture is represented in Fig. 5. The overall controllers and observers run on a ground PC. The desired spinning velocities of each propeller are sent at 500 [Hz] to the robot using a serial cable. The received velocity commands are then actuated by a controller (presented in [10]) running on the on-board ESC (Electronic Speed Control). The same serial communication is used to read at 1 [KHz] the IMU measurements that are then UKF-fused together with the motion capture system measurements (position and orientation of the quadrotor at 120 [Hz]) to obtain an estimation of the pose of the vehicle. The state estimation is then used to close the control loop and to get an estimation of the internal force along the link when the latter is taut.

The controller for the free-flight and tethered cases run in parallel and a supervisor, according to the state of the experiment, decides whose input has to be applied to the real system. The user input in the supervisor is needed to trigger situations of emergency.

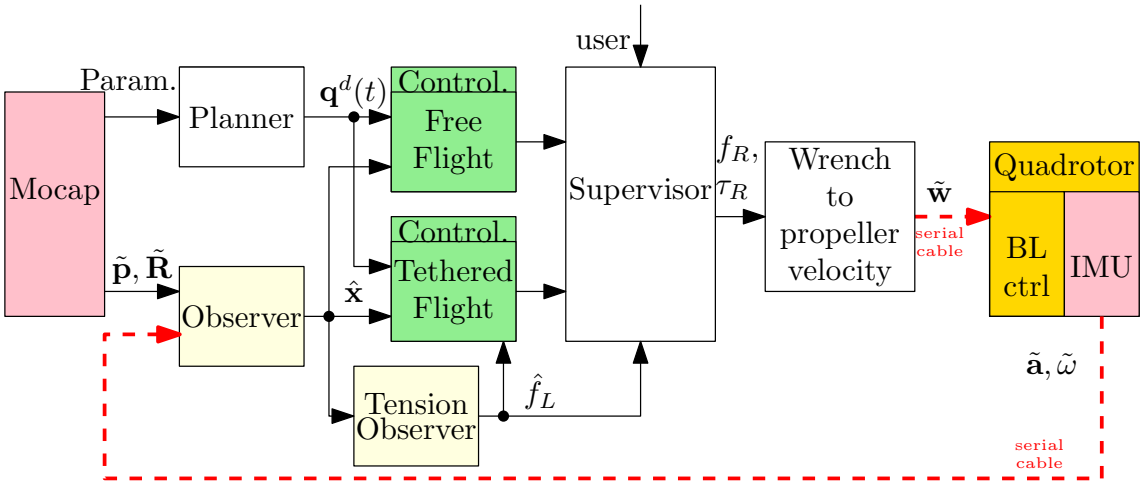

Figure 5: Schematic representation of the software architecture. Pink blocks represent the sensors. Green blocks represent the controllers and light yellow blocks represent the observers. Starting from the left, $\tilde{\mathbf{p}}$ and $\tilde{\mathbf{R}}$ represent the measured robot position and orientation, respectively; $\hat{\mathbf{x}}$ and $\hat{f}_L$ represent the estimated state and link internal force, respectively; $\mathbf{q}^d(t)$ represents the desired output trajectory; f_R and τ_R represents the input of the robot, i.e., thrust intensity and torque vector; $\tilde{\mathbf{w}}$ represents the desired spinning velocity of the propellers. Finally $\tilde{\mathbf{a}}$ and $\tilde{\omega}$ represent the readings of the IMU, i.e., specific acceleration and angular velocity.

3.5 Nonideality

Another practical aspect that has to be considered is the non-zero offset between the cable attaching point and the vehicle center of mass. Indeed the controller presented in [6] assumes that this offset is equal to zero. In this way the robot translational and rotational dynamics can be decoupled. However, this never happens in a practical case. Then, due to this non-zero offset, the internal force along the cable generates a torque on the vehicle that has to be carefully compensated. This is done computing the extra torque from the estimated tension and the estimated offset calculated with a mechanical analysis.

Finally we highlight the fact that the maximum tiling of the surface is bounded by the input limits. Indeed the more inclined is the slope, the less it is the thrust required to compensate the gravity close to the surface. Due to the impossibility of producing negative thrust for the single propeller, the almost zero total thrust implies a reduced control authority on the total input moment that may cause the instability of the attitude dynamics and of the whole system in general.

3.6 Experimental Results

In Fig. 3 and 6 the experimental results are shown. Figure 3 shows the first half of the experiment, i.e., the landing, by a series of images. In particular the first row shows the anchoring procedure done in a free-flight condition. On the other hand, the second row shows the actual execution of the tethered landing. A video of the full experiment is available at `https://www.youtube.com/watch?v=01UYN289YXk&t=7s`

Figure 6 shows the evolution of the state, outputs and inputs of the system during the landing and take-off maneuvers. At time zero the tethered controller is activated and the landing maneuver starts. At time t_L the landing is accomplished and the surface is reached. At time t_G the motors are stop to simulate the deploying of a robot/sensor. Finally, at time t_T the take-off maneuver starts.

From those plots one can see that the desired trajectory is tracked precisely, with only some small errors due to calibration errors. Despite the presence of tracking errors the landing and take-off maneuver are accomplished successfully and in a very safe and gentle way. This shows the big advantage of using a tether that makes the execution on the task reliable and robust to tracking and modeling errors.

Furthermore, notice that the intensity of the internal force along the link, defined by the symbol f_L, is always positive. This shows that the cable is kept taut for the whole execution of the maneuvers.

4 Conclusion

Despite its practical issues, the use of the tether and the presented control method, greatly increases the robustness and the reliability of the maneuver with respect to the free-flight method. However for the real application some improvement of the system has to be considered. For example a small winch could be added to unroll and roll-up the cable immediately before and after the tethered maneuvers. A more suitable anchoring mechanism can be designed according to the type of landing surface. Finally the robot could be equipped with a on-board vision system to identify the posi-

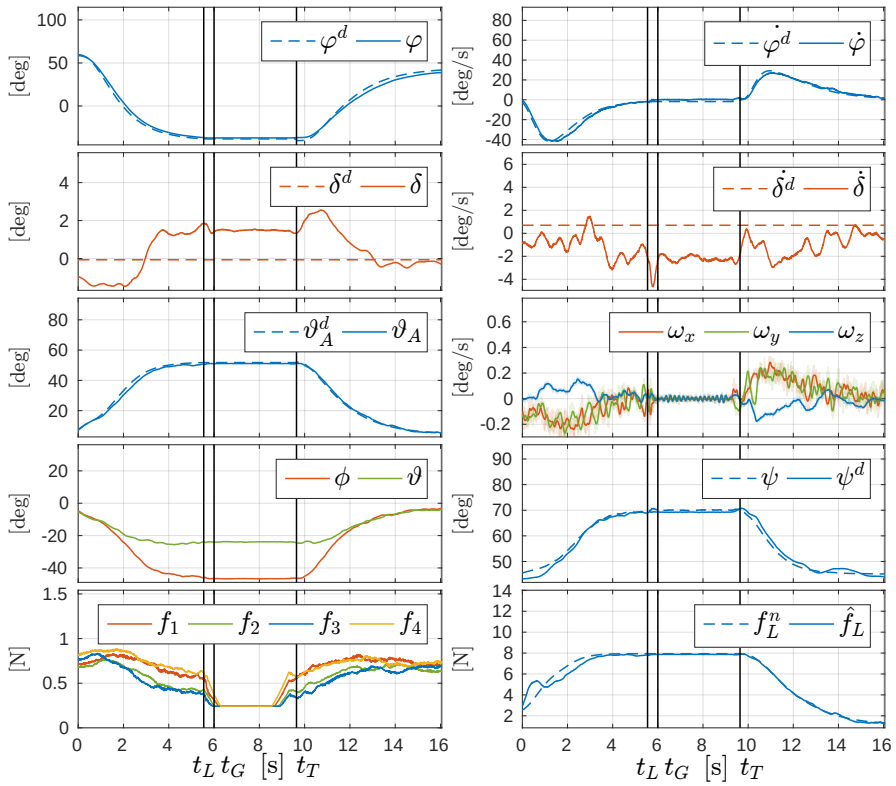

Figure 6: Plots of the state, outputs and inputs of the system during the tethered landing and take-off. In particular φ and δ describe the attitude on the cable and, given the link constraint, the position of the vehicle with respect to the anchoring point. ϑ_A is the angle between the robot and the link. ϕ and ψ are the angles that together with ϑ_A describe the orientation of the robot. f_1, f_2, f_3, f_4 are the forces produced by each propeller. Finally, f_L is the intensity of the internal force along the link. The super-script d and n represent the desired and the nominal values of the variable, respectively.

tion of anchoring point and the slope of the surface.

ACKNOWLEDGEMENTS

This research has been funded by the European Union's Horizon 2020 research and innovation program under grant agreement No 644271 AEROARMS.

REFERENCES

[1] D. Mellinger, N. Michael, and V. Kumar. Trajectory generation and control for precise aggressive maneuvers with quadrotors. *The Int. Journal of Robotics Research*, 31(5):664–674, 2012.

[2] M. Tognon and A. Franchi. Dynamics, control, and estimation for aerial robots tethered by cables or bars. *IEEE Trans. on Robotics*, 33(4):834–845, 2017.

[3] M. M. Nicotra, R. Naldi, and E. Garone. Nonlinear control of a tethered uav: The taut cable case. *Automatica*, 78:174 – 184, 2017.

[4] S. Lupashin and R. D'Andrea. Stabilization of a flying vehicle on a taut tether using inertial sensing. In *2013 IEEE/RSJ Int. Conf. on Intell. Robots and Systems*, pages 2432–2438, Tokyo, Japan, Nov 2013.

[5] M. Tognon, S. S. Dash, and A. Franchi. Observer-based control of position and tension for an aerial robot tethered to a moving platform. *IEEE Robotics and Autom. Letters*, 1(2):732–737, 2016.

[6] M. Tognon, A. Testa, E. Rossi, and A. Franchi. Take-off and landing on slopes via inclined hovering with a tethered aerial robot. In *2016 IEEE/RSJ Int. Conf. on Intelligent Robots and Systems*, pages 1702–1707, Daejeon, South Korea, Oct. 2016.

[7] M. Tognon and A. Franchi. Position tracking control for an aerial robot passively tethered to an independently moving platform. In *20th IFAC World Congress*, Toulouse, France, Jul. 2017.

[8] L.A Sandino, D. Santamaria, M. Bejar, A. Viguria, K. Kondak, and A. Ollero. Tether-guided landing of unmanned helicopters without GPS sensors. In *2014 IEEE*

Int. Conf. on Robotics and Automation, pages 3096–3101, Hong Kong, China, May 2014.

[9] G. Gioioso, M. Ryll, D. Prattichizzo, H. H. Bülthoff, and A. Franchi. Turning a near-hovering controlled quadrotor into a 3D force effector. In *2014 IEEE Int. Conf. on Robotics and Automation*, pages 6278–6284, Hong Kong, China, May. 2014.

[10] A. Franchi and A. Mallet. Adaptive closed-loop speed control of BLDC motors with applications to multi-rotor aerial vehicles. In *2017 IEEE Int. Conf. on Robotics and Automation*, Singapore, May 2017.